Multi-layer GNSS and LEO-PNT Positioning: Integrity under Constellations' Correlation

J. Duník, I. Punčochář, L. Král, O. Straka
Dept. of Cyber., Univ. of West Bohemia
Univerzitní 8, 306 14 Pilsen, Czech Rep.
Email: {dunikj, ladkral, ivop, straka30}@kky.zcu.cz

O. Daniel
HULD, s.r.o.
nám. W. Churchilla 1800/2, 130 00 Prague, Czech Rep.
Email: ondrej.daniel@huld.io

F. S. Prol, M. Liaquat, M. Z. H. Bhuiyan
Navi. Dept., Finnish Geospatial Research Institute
National Land Survey of Finland
02150, Espoo, Finland
Email: {fabricio.dossantosprol, muwahida.liaquat, zahidul.bhuiyan}@nls.fi

***Abstract*—This paper deals with the initial integrity evaluation of the navigation information provided by the multi-layer GNSS and LEO-PNT constellation. Although, the global satellite navigation systems (GNSS) play indispensable role in almost all aspects of today's society, their signals are prone to intentional or accidental interference. Therefore, low Earth orbit (LEO) constellations aiming at position, navigation, and timing (PNT) solution have recently been introduced as their extension. The LEO-PNT constellations are planned to contain *hundreds* of SVs with better interference resilience and geometric *diversity*. As a consequence, the multi-layer GNSS and LEO-PNT constellation was shown to offer more accurate PNT solution. In this paper, we focus on another important aspect of the multi-layer navigation information, which is its integrity assessment. In particular, we analyse possible dependencies between GNSS and LEO-PNT constellations and their impact on the integrity evaluated using the solution separation. The analysis is supported by the numerical simulations using GPS and LEO-PNT constellations with 32 and 441 satellites, respectively.**

Keywords: GNSS; LEO-PNT; Integrity monitoring; PHMI allocation; Measurement noise; Interference resilience.

I. Introduction

Global navigation satellite systems (GNSS), such as Galileo or GPS, provide position, navigation, and timing (PNT) solutions based on signals from tens of satellites (or space vehicles (SVs)) orbiting at altitudes about 20,000 km for GPS and about 23,000 km for Galileo. Although the GNSS play an indispensable role in almost all aspects of today's society, their signals are prone to intentional or accidental interference due to occlusion, multipath, or jamming and spoofing. Therefore, low Earth orbit (LEO) constellations aiming at PNT, such as Xona, Iridium, CentiSpace, or Geespace, have recently been introduced as an alternative to or extension of the GNSS. The LEO-PNT constellations are planned to contain *hundreds* of SVs, which will orbit at altitude about 1000 km [12].

As the LEO-PNT constellation SVs will orbit significantly closer to the users (typically 20 times closer than GNSS), they will provide stronger transmitted signal power, leading to higher positioning *accuracy*, higher resilience to various forms of attacks known from the GNSS world, and seamless positioning experience even in indoor environments. Due to faster dynamics in LEO orbit and smaller footprints on the user side, the constellation must contain many satellites to provide global coverage. The fast motion of the LEO satellites contributes significantly to the geometric diversity (compared with the traditional GNSS constellations), allowing for rapid convergence of the precise point positioning (PPP) techniques. Another advantage of the LEO-PNT is that the LEO-PNT measurements can be processed with the same algorithms used for the GNSS measurement (including integration with other sensors such as the inertial measurement unit or barometric altimeter).

On the other hand, the LEO-PNT will not, at least in the initial phase, be equipped with high-quality clocks, such as GNSS-grade atomic clocks, which are needed to provide high-accuracy positioning and timing services. Instead, the currently considered LEO-PNT constellations will derive their timing and positioning capabilities from the existing GNSS constellations. Therefore, there is a need for close-to-real-time GNSS-based precise orbit determination algorithms implemented on the LEO-PNT satellites [12].

Due to this dependency of the LEO-PNT on GNSS, the combined LEO-PNT and GNSS positioning architecture is typically denoted as multi-layer PNT architecture since the particular constellations form "layer" as illustrated in Figure 1. Compared to the GNSS constellations (that are independently maintained), the envisioned multi-layer constellation will *positively* impact the accuracy of the PNT solution (in terms of *lower* estimate error covariance matrix). Despite the lower error covariance matrix, the integrity of the navigation information can *adversely* impact the provided protection levels (PLs) due to

- Higher number of visible SVs (both GNSS and LEO-PNT) generally leading to increased number of faults,

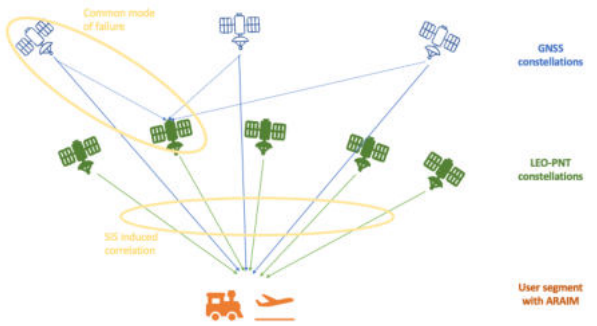

Figure 1: Multi-Layer PNT service (with indication of common faults).

- Correlation among the GNSS and LEO-PNT measurements given not only due to the LEO SV PNT solution derived from the GNSS, but also due to signal-in-space measurement noise correlation.

Higher PLs might be problematic, especially for areas with stringent requirements on navigation information quality.

Whereas the performance of the multi-layer GNSS and LEO-PNT has been evaluated in terms of the accuracy [12], its performance in terms of the integrity has been somewhat overlooked, although the integrity is an *essential* parameter to be met not only in general aviation but also in other transport domains such as urban air mobility (UAM). In the literature, a few studies discussing the integrity of the multi-layer architecture can be found in [16], [17]; unfortunately, without an analysis of the impact of the GNSS and LEO-PNT dependency on a number and probability of possible faults. As will be shown, the fault number and dependency significantly affect the design of the integrity monitoring algorithms and calculated PLs.

In this paper, we *(i)* specify and analyse the dependency between GNSS and LEO-PNT faults, *(ii)* propose an allocation of the probabilities of false alarm and hazardous misleading information, measurement noise properties, and *(iii)* evaluate their impact on integrity (and resulting PLs) using the solution separation concept. The discussed concept is then evaluated in a numerical study using a scenario with the GPS constellation and a LEO-PNT constellation, which gives an idea about the benefit of the LEO-PNT integration with the GNSS.

The rest of the paper is organised as follows. Section II reviews the position estimation and noise properties for the GPS and proposed for the LEO-PNT. The accuracy and integrity of the position solution are discussed in Section III, together with constellation-related fault probabilities. The hazardous misleading information and the integrity monitoring method are treated in Sections IV and V. The discussed algorithms are numerically verified in Section VI, and the concluding remarks are given in Section VII.

II. Position Estimate and Measurement Noise Properties

The satellite-based navigation systems estimate receiver position (and other navigation parameters if required) based on time-of-arrival measurements characterising the distances between the receiver with unknown sought position and SVs with known positions. The distance, denoted as a pseudorange, $\rho^{(i)}$ can be then written as [1], [6]

$$\rho^{(i)} = \|\mathbf{s}^{(i)} - \mathbf{p}\| + \Delta_t + v^{(i)}, i = 1, 2, ..., N, \quad (1)$$

where $\mathbf{s}^{(i)}$ is a known position of i-th SV, $\mathbf{p}$ is the unknown receiver position, Δ_t is the off-set caused by the receiver clock error, and $v^{(i)}$ is a zero-mean measurement noise with variance $(\sigma^{(i)})^2$ with components detailed later.

Estimation of unknown receiver position and clock error(s)[1] for m GNSS constellations, i.e., of $\mathbf{x} = [\mathbf{p}^T, \mathbf{\Delta}_t]^T$, is typically based on linearised system of equations (1), $\forall i$, which reads [1]

$$\mathbf{y} = \mathbf{H}\Delta\mathbf{x} + \mathbf{v}, \quad (2)$$

where

- $\mathbf{y} \in \mathbb{R}^N$ is a known vector of pseudoranges compensated for all available corrections, e.g., atmospheric delay, satellite clock error, and the first term of range equation Taylor expansion,
- $\mathbf{H} \in \mathbb{R}^{N\times 3+m}$ is a known matrix of *(i)* unit line-of-sight vectors aiming from the receiver to the SVs (first three columns) and *(ii)* indication of the constellation for the particular SV (last m columns),
- $\Delta\mathbf{x} \in \mathbb{R}^{3+m} = \mathbf{x} - \bar{\mathbf{x}}$ is the *unknown* (and *sought*) difference between actual receiver position and clock offset and its initial estimate determining the linearisation point $\bar{\mathbf{x}}$, and
- $\mathbf{v} = [v^{(1)}, v^{(2)}, \ldots, v^{(N)}]$ is the concatenated measurement noise vector with the covariance matrix $\mathbf{R} = \mathsf{cov}[\mathbf{v}]$.

The weighted least-squares estimate of the difference becomes

$$\Delta\hat{\mathbf{x}} = \left(\mathbf{H}^T\mathbf{W}\mathbf{H}\right)^{-1}\mathbf{H}^T\mathbf{W}\mathbf{y}, \quad (3)$$

where the weighting matrix is $\mathbf{W} = \mathbf{R}^{-1}$, and the estimated receiver position and receiver clock drift (with respect to one or more constellations) is $\hat{\mathbf{x}} = \bar{\mathbf{x}} + \Delta\hat{\mathbf{x}}$. The estimate error covariance matrix reads

$$\mathbf{C} = \left(\mathbf{H}^T\mathbf{W}\mathbf{H}\right)^{-1}. \quad (4)$$

Calculation of the LS solution (3) is conditioned by the knowledge of the measurement noise covariance matrix $\mathbf{R}$. Typically, the matrix is supposed to be diagonal, with the variances defined as follows.

[1] As the time base is not synchronised over m GNSS constellations, it is necessary to estimate clock error for each processed constellation.

A. GPS Measurement Noise Variance

The measurement noise variance of the GPS compensated pseudorange for a dual-frequency receiver is given by [1], [7], [15]

$$\mathbf{R}(i,i) = (\sigma^{(i)})^2 = (\sigma^{(i)}_{\mathrm{URA/URE}})^2 + (\sigma^{(i)}_{\mathrm{tropo}})^2 + (\sigma^{(i)}_{\mathrm{user}})^2, \tag{5}$$

where

- $\sigma^{(i)}_{\mathrm{URA}} = 0.75m$ and $\sigma^{(i)}_{\mathrm{URE}} = 0.5m$ stand for the standard deviation (STD) of the clock and ephemeris error of i-th GPS SV used for integrity calculation (denoted as *user range accuracy*) and for the accuracy and continuity calculation (denoted as *user range error*), respectively,
- $\sigma^{(i)}_{\mathrm{tropo}} = 0.12\frac{1.001}{\sqrt{0.002001+\left(\sin(\frac{\pi\theta}{180})\right)^2}}[m]$ is a residual tropospheric error (or delay) STD of i-th GPS SV with elevation $\theta[deg]$,
- $\sigma^{(i)}_{\mathrm{user}} = \sqrt{\frac{f^4_{\mathrm{L1}}+f^4_{\mathrm{L5}}}{(f^2_{\mathrm{L1}}-f^2_{\mathrm{L5}})^2}}\sqrt{(\sigma^{(i)}_{\mathrm{MP}})^2 + (\sigma^{(i)}_{\mathrm{noise}})^2}[m]$ is the user/receiver error STD being function of (dual) frequencies of L1 and L5 signals and smoothed multipath and receiver noise STDs defined as $\sigma^{(i)}_{\mathrm{MP}} = 0.13 + 0.53\exp(-\theta/10)$ and $\sigma^{(i)}_{\mathrm{noise}} = 0.15 + 0.43\exp(-\theta/6.9)$, respectively.

B. LEO-PNT Measurement Noise Variance

The definition of the representative measurement noise error budget for LEO-PNT is much more challenging as there is no standard or widely accepted definition. However, in [18] the authors provided an *initial* measurement noise assessment of the Luojia-1A SV[2]. The LEO-PNT pseudorange measurement STD seems to be below 1 meter (compared to several of meters for GPS or GNSS SV in general). The lower measurement noise STD of the LEO-PNT is expected as the LEO-PNT SVs are located significantly closer to the Earth surface [12].

However, due to the *missing* comprehensive evaluation of the expected LEO-PNT measurement noise, the LEO-PNT measurement noise STD is, in *this* paper, considered as a slightly down-scaled GPS error budget, i.e.,

$$\mathbf{R}(i,i) = c^2\left((\sigma^{(i)}_{\mathrm{URA/URE}})^2 + (\sigma^{(i)}_{\mathrm{tropo}})^2 + (\sigma^{(i)}_{\mathrm{user}})^2\right), \tag{6}$$

with the scaling factor[3] $c = 0.9$. Note that this study does not consider the fault-free range biases [7].

III. Navigation Information Performance Metrics

A considered navigation system provides (at least) an estimate of the receiver position using statistical processing of the GPS and LEO-PNT measured pseudoranges. The estimated position, often denoted as the navigation information, is used in many applications, including safety-related ones, where the quality of the information has to be quantified. We can mention and briefly define the following widely used performance metrics [5], [7], [8]:

- *Integrity* is a measure of the trust that can be placed in the correctness of the information supplied by the total (navigation) system. Integrity includes the ability of a system to provide timely and valid warnings to the user (alerts). Evaluated integrity parameters are
  - Integrity risk is the probability that the estimated navigation information error exceeds an alert/required limit.
  - PL is bound, for which it is guaranteed that the probability of the error exceeding the PL is smaller than or equal to the integrity risk. PL and integrity risk are, in the sense of integrity assessment, interchangeable.
  - Alert limit is the error tolerance not to be exceeded without issuing an alert.
  - Time-to-alert is the maximum allowable time elapsed from the onset of the navigation system being out of tolerance until the alert.
- *Accuracy* is a measure or the statistical description of the estimated navigation information error.
- *Continuity* is the ability of the total system to perform its function without interruption during the intended operation.
- *Availability* of a navigation system is the ability of the system to provide the required function and performance at the initiation of the intended operation.

This paper focuses on the integrity and accuracy assessment of the estimated position. Whereas the accuracy is assessed simply by the position estimate (root) mean square error or the respective covariance matrix and bias, the integrity statistical definition is more involved.

A. Integrity

Integrity quantifies the impact of undetected faults on the navigation information estimation error. In order to avoid making assumptions on unknown fault distributions, the integrity risk of a worst-case fault is evaluated in terms of the probability of hazardous misleading information (HMI). The HMI is defined as a probability that the navigation information error exceeds the alert limit while not being detected by a fault detection algorithm. In other words, the required probability is defined as [7]

$$P_{\mathrm{HMI}} = P(|\varepsilon(j)| > L, q < T), \tag{7}$$

where $\varepsilon(j) = \mathbf{x}(j) - \hat{\mathbf{x}}(j)$ is the error of the j-th position estimate or its function, L is the allowed limit (e.g., required vertical or horizontal PL denoted as VPL or HPL, respectively), q is a test statistic of the detection algorithm, and T is a detection threshold (calculated from the estimate error covariance matrix $\mathbf{C}$).

[2]Luojia-1 is an Earth observation SV built by the Wuhan University (https://space.skyrocket.de/doc_sdat/luojia-1.htm).

[3]In [9], the more conservative scaling factor $c = 1.5$ was considered for the opportunistic LEO-related measurements, which are not primarily intended for navigation.

Considering the set of f mutually exclusive fault hypotheses $\{H_i\}_{i=1}^{f}$, the integrity risk reads

$$P_{\mathrm{HMI}} = \sum_{i=1}^{f} P(|\varepsilon(j)| > L, q < T|H_i)P(H_i) = \sum_{i=1}^{f} P(\mathrm{HMI}|H_i)P(H_i), \quad (8)$$

where $P(H_i)$ is a priori known probability of the related fault occurrence. As f can be too high for evaluation, $P(H_i)$ for certain faults is negligible compared to required P_{HMI}, or some faults cannot be detected (such as failure of all SVs), the number of hypotheses to be monitored can be *reduced* such as

$$P_{\mathrm{HMI}} \leq \sum_{i=1}^{h} P(\mathrm{HMI}|H_i)P(H_i) + P_{\mathrm{notMonitored}}, \quad (9)$$

where $P_{\mathrm{notMonitored}} = \sum_{i=h+1}^{f} P(\mathrm{HMI}|H_i)P(H_i) \leq \sum_{i=h+1}^{f} P(H_i)$.

A careful definition of the fault hypothesis and the probabilities $P(H_i), \forall i$, is thus of paramount importance.

B. GNSS and LEO-PNT Faults and their Probabilities

The faults hypotheses considered in the area of GPS (autonomous) integrity monitoring are mostly related to the *narrow* failure (i.e., failure of one SV) with

$$P(H_{\mathrm{GPSnarrow}}) = 10^{-5} \quad (10)$$

or *wide* failure (i.e., failure of a whole constellation)

$$P(H_{\mathrm{GPSwide}}) = 10^{-8}. \quad (11)$$

These probabilities stem from the analysis of past data.

Unfortunately, such probabilities are unavailable for the LEO-PNT SVs and the constellation due to a lack of data. Therefore, we will introduce and briefly discuss two possible scenarios, which differ in *dependency* of GPS and LEO-PNT constellations (illustrated in Figure 1);

1) Independent Constellations: By the term independent, we mean that the LEO-PNT SV PNT information is determined independently of the GNSS constellation used for combination in the user receiver. For example, LEO-PNT SV can be positioned without the need for the GNSS, or it uses GPS, but the receiver tracks Galileo SVs in addition to the LEO-PNT SVs.

2) Dependent Constellations: Dependent constellations are those where a LEO-PNT SV calculates its PNT information based on GNSS measurements. Then, the user receiver combines LEO-PNT and GNSS measurements without a notion of their correlation.

C. Considered Scenario and Probabilities

Unknown dependency of GNSS and LEO-PNT constellations effectively prevents standard calculations used in the integrity monitoring domain. The reason is that failure of one GNSS SV can cause failure of multiple LEO-PNT SVs, which means that failures of particular SVs are *not* mutually exclusive. On the other hand, the assumption of LEO-PNT SV positioning without the need for the GNSS seems to be optimistic, at least in the near future.

Therefore, a realistic scenario selected in this paper is that the LEO-PNT SV calculates its position (and time correction) based on one GNSS constellation, such as Galileo, and the user receiver combines these LEO-PNT measurements with the GPS pseudoranges. Then, the probability of LEO-PNT narrow failure is, in this paper, considered as

$$P(H_{\mathrm{LEOnarrow}}) = n \times 10^{-5}, \quad (12)$$

where n shall respect the number of used Galileo SVs for positioning of the LEO-PNT SV and employed fault detection (FD). In this paper, we consider $n = 2$. The probability of LEO-PNT-wide failure is considered as

$$P(H_{\mathrm{LEOwide}}) = 2 \times 10^{-8}, \quad (13)$$

motivated by the fact the Galileo and LEO-PNT constellations can fail with the same probability 10^{-8}.

We should stress that we *neglect* correlation caused by the Galileo SVs in LEO-PNT SV positioning, which means that narrow failure of one LEO-PNT SV can be correlated with failure of another LEO-PNT SV via a common Galileo measurement(s). The intuition behind this approximation is that the Galileo constellation can be monitored either at the receiver level or LEO-PNT SV level to detect the faults and minimise the correlation between LEO-PNT SV faults.

Similarly to the specification of noise properties, the probability allocation will be thoroughly discussed and analysed once the planned constellations become active and the hardware and software architecture is fixed.

IV. Probability of Hazardous Misleading Information Allocation

Integrity monitoring methods rely on allocating P_{HMI} budget among the monitored faults and specification of $P_{\mathrm{notMonitored}}$. Two allocation schemes can be designed

- *Fixed*, which depends only on the number of hypotheses h [2], [8],
- *Optimal*, which depends besides on h also on constellation layout and calculated estimate covariance matrices [1].

Due to lower computational complexity and since this paper presents an initial concept of LEO-PNT and GPS integration, we further focus on the fixed scheme.

Within the fixed schemes, we will focus on a *standard* scheme referring to an algorithm of the advanced receiver autonomous integrity monitoring [5], which does not account for multiple simultaneous faults. It means the single SV faults with probabilities $P(H_{\mathrm{GPSnarrow}})$ (10) and $P(H_{\mathrm{LEOnarrow}})$ (12) are monitored and the remaining constellation and simultaneous faults are not. These un-

monitored probabilities form the *upper bound* probability $P_{\text{notMonitored}}$, which is thus defined as

$$P_{\text{notMonitored}} = P(H_{\text{GPSwide}}) + P(H_{\text{LEOwide}}) + \binom{N_{\text{GPS}}}{2}(P(H_{\text{GPSnarrow}}))^2 + \binom{N_{\text{LEO}}}{2}(P(H_{\text{LEOnarrow}}))^2 + N_{\text{GPS}}N_{\text{LEO}}P(H_{\text{GPSnarrow}})P(H_{\text{LEOnarrow}}), \quad (14)$$

where N_{GPS} is a number of tracked GPS satellites and N_{LEO} is a number of tracked LEO-PNT satellites so that $N = N_{\text{GPS}} + N_{\text{LEO}}$. The 3rd, 4th, and 5th right-hand side addends take into account the simultaneous failure of two SVs (two GPS SVs, two LEO-PNT SVs, and a combination of one GPS SV and one LEO-PNT Sv). The probability of simultaneous failure of three or more satellites is negligible w.r.t. typically considered $P_{\text{HMI,rem}}$.

The resulting $P_{\text{HMI,rem}}$, which is allocated among the monitored single fault hypotheses by the integrity monitoring algorithm, is then given as

$$P_{\text{HMI,rem}} = P_{\text{HMI}} - P_{\text{notMonitored}}. \quad (15)$$

V. Integrity Monitoring by Solution Separation

Integrity monitoring methods for the (horizontal) position domain have been pioneered in the aviation industry since the beginning of the utilisation of the GPS for en-route navigation back in the 1990s. As no augmentation systems were available, the integrity had to be solved by the GPS receiver itself, which gave rise to the methods known as the (advanced) receiver autonomous integrity monitoring methods (ARAIM) [3], [4], [7], [10], [19]. These methods can be classified into two groups:

- *Measurement* domain, where the fault detection (FD) algorithm is based on a statistical analysis of the measurement residuals [4].
- *State* domain, where the FD is based on a statistical analysis of the difference between the state estimate computed using all measurements and estimates computed using sub-sets of measurements. A prominent example of this approach is the solution separation (SolSep) method [3], [5].

As both approaches provide similar performance, we will focus on SolSep in this paper, which can be easily extended for mitigation of any type of fault.

The SolSep method is based on a statistical comparison position estimate (3), (4) calculated using all available pseudorange measurements $\rho^{(i)}, \forall i$, (1) with an estimate based on a subset of measurements. The former estimate is denoted as the full-solution, and the latter as the sub-solution. The sub-solutions are defined to reflect the fault to be mitigated.

A. Solutions Definition

Let the position full-solution processing all N measurements (3), (4) consisting of the estimate and the associated estimate error covariance matrix be denoted as

$$\Delta\hat{\mathbf{x}}_0, \mathbf{C}_0. \quad (16)$$

Assuming a *single* SV fault, we can define N sub-solutions, where each sub-solution processes a *unique* subset of $N-1$ pseudorange measurements. The sub-solution estimate is denoted as

$$\Delta\hat{\mathbf{x}}_n, \mathbf{C}_n, n = 1, 2, \ldots, N. \quad (17)$$

Then, there is always one sub-solution not affected by this fault. Thus, by statistically comparing the full- and sub-solutions estimates, we can detect a fault and calculate the PL. In the following subsections, we illustrate the SolSep for HPL calculation. The VPL is calculated analogously [5], [7].

B. Test Statistic and Decision Threshold

If the estimated position correction is in the navigation (tangential) frame [6], then the first two elements of $\Delta\hat{\mathbf{x}}$, i.e., $\Delta\hat{\mathbf{x}}^{\text{H}}$, represent the correction to the horizontal position. The SolSep test statistic (or discriminator/separation) is, then, defined as

$$\mathbf{d}_n^{\text{H}} = \Delta\hat{\mathbf{x}}_0^{\text{H}} - \Delta\hat{\mathbf{x}}_n^{\text{H}}, \forall n. \quad (18)$$

In the fault-free case, the statistic is a zero-mean random variable with the covariance matrix

$$d\mathbf{C}_n^{\text{H}} = \mathsf{E}[(\Delta\hat{\mathbf{x}}_0^{\text{H}} - \Delta\hat{\mathbf{x}}_n^{\text{H}})(\Delta\hat{\mathbf{x}}_0^{\text{H}} - \Delta\hat{\mathbf{x}}_n^{\text{H}})^T] = \mathbf{C}_n - \mathbf{C}_0, \quad (19)$$

if certain (but weak) assumptions are met [19]. Then, the fault is detected, and the alert is raised if

$$d_n^{\text{H}} > D_n^{\text{H}}, \quad (20)$$

where $d_n^{\text{H}} = \|\mathbf{d}_n^{\text{H}}\|$ is the Euclidean norm of (18). The decision threshold is defined

$$D_n^{\text{H}} = K_{\text{FA}}^n \sqrt{\lambda^{d\mathbf{C}_n^{\text{H}}}}, \quad (21)$$

where K_{FA}^n is a multiplication coefficient depending on the probability of false alarm P_{FA} allocated for the given sub-solution (and hypotheses) and $\lambda^{d\mathbf{C}_n}$ is the maximum eigenvalue of $d\mathbf{C}_n$. Detailed relations for K_{FA}^n calculation, P_{FA} allocation, and compensation for the second eigenvalue of $d\mathbf{C}_n$ can be found in [11].

C. Protection Level

The PL of the horizontal position (HPL) is calculated as

$$HPL = \max\{HPL_1, HPL_2, \ldots, HPL_N\}, \quad (22)$$

where $PL_n = D_n^{\text{H}} + a_n^{\text{H}}$ and the term

$$a_n^{\text{H}} = K_{\text{MD}} \sqrt{\lambda^{\mathbf{C}_n^{\text{H}}}}, \quad (23)$$

represents the uncertainty of n-th sub-solution horizontal position covariance matrix $\mathbf{C}_n^{\text{H}}$ and allocated probability of missed detection P_{MD}. The probability P_{MD} is derived from $P_{\text{HMI,rem}}$ (15) and $P(H_i)$ considered in (9)–(13). The calculated HPL can be thus imagined as a circular area centred as the full-solution position estimate with a radius given by the maximum of the sum of the separation threshold D_n and the term a_n as illustrated in Figure 2.

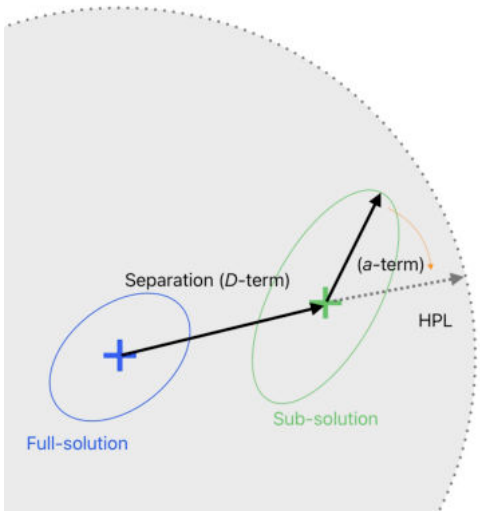

Figure 2: Full-solution, sub-solution, and HPL illustration.

VI. Numerical Simulation

The discussed concept of the multi-layer GPS and LEO-PNT constellation is simulated and the accuracy and integrity of the positioning information is evaluated. The details on simulation configuration can be found in the next sub-sections.

A. Constellation Simulator

In this study, we utilised LEO-S9 (LEO simulator with 9 modules), a simulation tool developed for the strategic planning of GNSS-like constellations within LEO altitudes [13], [14]. It allows the replication of the space, ground, and user segments, in addition to the atmospheric and Earth effects on the signal propagation. Main simulated parameters include orbit errors, clock offsets, phase centre offsets (PCO), phase centre variations (PCV), instrumental biases, such as the differential code bias (DCB), atmospheric refraction (ionosphere and troposphere), phase wind-up, and relativistic effects.

The constellation was simulated considering a LEO-PNT mission over a 12-hour observational period with sampling $1[sec]$. This was performed with an orbit altitude of 800 km and 441 satellites since it allowed to keep the geometric dilution of precision (GDOP) lower than four, which is an excellent geometry for further analysis. The simulated mission aimed to mimic real-world scenarios by providing precise orbit models, including the Cowell numerical integration for orbit propagation considering the Earth's gravity field, J2 perturbation due to the Earth's shape, third body effects, solar radiation pressure, and atmospheric drags.

The simulations also include GNSS satellites to characterise a multi-layer constellation completely. To this end, precise products generated by the International GNSS Service (IGS) are used as a basis. They provided high-accuracy GPS orbits with a time-interval period of 5 minutes. The GPS satellite orbits were obtained every 1 second by a moving-window Lagrange polynomial interpolation into the Earth-centred inertial (ECI) frame, which is a typical interpolation technique to provide sub *cm* accuracy.

θ		hSTD	vSTD	HPL	VPL
10	GL	0.31(±0.02)	0.74(±0.14)	2.86(±0.32)	6.34(±1.23)
	G	0.66(±0.13)	1.22(±0.21)	8.15(±2.69)	11.81(±4.15)
	L	0.37(±0.05)	1.10(±0.42)	4.62(±1.84)	13.67(±7.95)
15	GL	0.35(±0.10)	0.96(±0.25)	4.72(±1.92)	10.34(±3.20)
	G	0.74(±0.18)	1.45(±0.37)	12.07(±6.80)	18.77(±13.80)
25	GL	0.55(±0.19)	1.63(±0.44)	9.16(±13.66)	20.18(±28.98)
	G	1.02(±0.35)	1.96(±0.40)	23.1(±16.25)	36.86(±28.89)

Table I: Positioning performance – L: LEO-PNT, G: GPS.

θ	10	15	25
GPS	9.35	7.13	6.31
LEO-PNT	10.21	5.78	4.44

Table II: Expected number of visible SVs.

By employing LEO-S9, we could simulate satellite constellations and precisely model the dynamics of LEO and GPS orbits, enabling us to provide pseudorange measurements and covariance matrices to a ground-based user.

B. Scenario Definition: Independent Constellations

In this paper, we evaluate the position estimate of a stationary receiver located at *latitude* $49°44'53.0''$N and longitude $13°22'27.0''$E assuming the GPS and the LEO-PNT measurement noise models and failure probabilities defined above. For integrity, we assume the total HMI budget to be $P_{\text{HMI}} = 2 \times 10^{-7}$ equally split among horizontal and vertical channels. The remaining HMI budget $P_{\text{HMI,rem}}$ (15) is allocated among the sub-solutions according to the particular probabilities $P(H_i)$ of the failures to be mitigated. The probability of false alarm P_{FA} is allocated equally among the sub-solutions.

The position estimate, transformed into the navigation frame, was evaluated using the following criteria

- Accuracy in the form of STD (based on the calculated covariance matrix $\mathbf{C}$ (4)) for horizontal and vertical positions further denoted as $hSTD_k$ and $vSTD_k$, respectively,
- Integrity in the form of PL (calculated by the SolSep) for horizontal and vertical channels denoted as HPL_k and VPL_k, respectively,

for each time instant $k = 1, \ldots, T, T = 43200$. The number of visible SVs of both constellations was recorded as well. The overall quality for both criteria was assessed using the *sample* mean and STD over all time instants k. The overall STDs and PLs are summarised in Table I for

- Varying mask angle θ,
- Processing GPS+LEO-PNT, GPS only, and LEO-PNT only measurements.

The average number of visible SV for each constellation is given in Table II. For illustration, the time behaviour of the considered quantities can be found in Figures 3 and 4 for $\theta = 15[deg]$ and $\theta = 25[deg]$, respectively, for a shorter window. Note that, for $\theta = 25[deg]$, LEO-PNT does not allow calculating the position solution due to the low number of SVs. For the sake of completeness, dependency

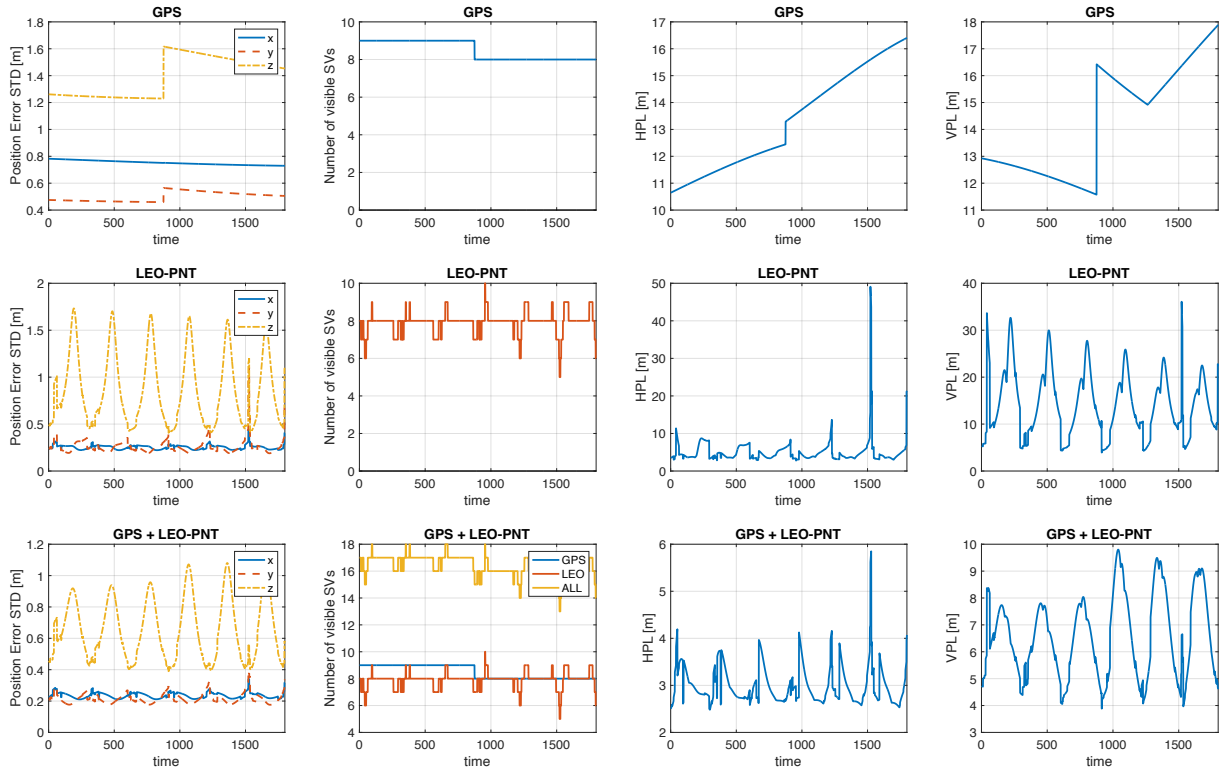

Figure 3: Positioning performance (mask angle $\theta = 15$ $[deg]$).

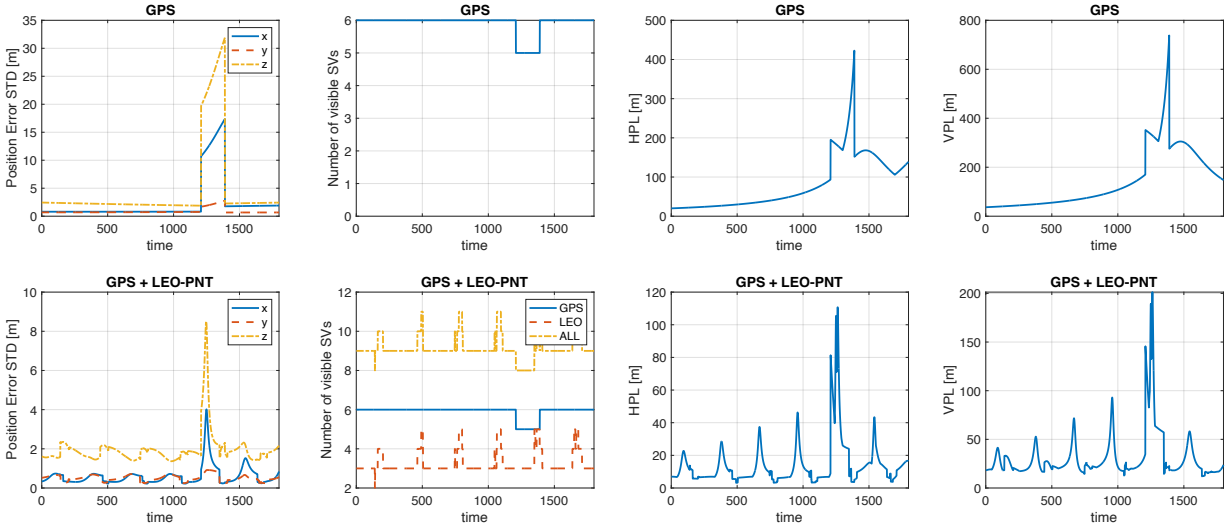

Figure 4: Positioning performance (mask angle $\theta = 25$ $[deg]$).

of averaged VPL and HPL on the LEO-PNT measurement noise variance via the scaling parameter c (6) is illustrated in Figure 5.

C. Observations and Open Questions

The results, summarised in Figures 3, 4 and Tables I, II, lead to following observations:

- Compared to GPS-only positioning, GPS+LEO-PNT significantly improves accuracy and integrity (more than 50%, observed from Table I). Improvement w.r.t. LEO-PNT-only positioning is rather modest.

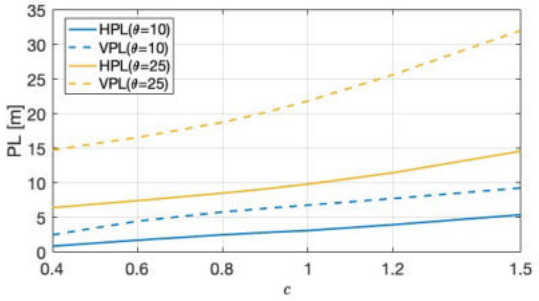

Figure 5: Dependency of *average* PL on LEO-PNT noise properties.

- For masking angle $\theta > 10$, the LEO-PNT cannot be used independently of a GNSS constellation due to the low number of visible SV needed for integrity-related calculation. This is a fundamental observation for using LEO-PNT in urban areas (with a high masking angle).
- For $\theta > 35$, GPS+LEO-PNT does not provide a sufficient number of visible SVs for integrity-related calculation. Another GNSS constellation shall be employed to solve this deficiency issue, which might affect the correlation between constellations' faults.
- LEO-PNT provides highly varying accuracy and integrity, given by the rapid change in constellation geometry. On the other hand, in the LEO-PNT results, we do not observe sudden jumps caused by adding or removing GPS SV.

The observations are valid for the *considered* scenario under assumed models and constellation faults. For overall conclusion, the following areas and tasks shall be explored

- Realistic models of LEO-PNT measurement noise and SV failure probabilities,
- Correlation between LEO-PNT and GNSS signal-in-space errors,
- For low mask angles θ, the positioning algorithm can be equipped with a *geometry screening*. The preliminary simulations show that removing two SVs from each constellation leads to a rather marginal degradation of positioning performance.
- For a higher narrow failure probability of a LEO-PNT SV, ARAIM with dual fault monitoring shall be considered, which increases the computational complexity.
- To smooth the high variability of LEO-PNT-based solution caused by rapid constellation change, an integration with an inertial navigation system or other sensors such as a barometric altimeter or odometer shall be considered.

VII. Concluding Remarks

The paper assessed the positioning performance of the multi-layer constellation, which combines the current GPS and envisioned LEO-PNT constellations. The emphasis was laid on the constellations' properties, the constellation fault dependency, and their impact on the positioning integrity. The considered models were evaluated in a numerical study showing the benefits and limitations of the multi-layer architecture.

Acknowledgement: J. Duník, I. Punčochář, L. Král, and O. Straka's work was supported by National Competence Center under Grant BOVENAC TN 02000054. F. S. Prol, M. Liaquat, and M. Z. H. Bhuiyan were supported by the INdoor Navigation from CUBesAT Technology (INCUBATE) project through the Technology Industries of Finland Centennial Foundation and the Jane and Aatos Erkko Foundation (JAES).

References

[1] Blanch, J., Walter, T., Enge, P., Lee, Y., Pervan, B., Rippl, M., Spletter, A.: Advanced RAIM user algorithm description: Integrity support message processing, fault detection, exclusion, and protection level calculation. In: Proceedings of the 25th International Technical Meeting of The Satellite Division of the Institute of Navigation, Nashville, TN (September 2012)

[2] Blanch, J., Walter, T., Enge, P., Wallner, S., Fernandez, F., Dellago, R., Ioannides, R., Pervan, B., Fernandez-Hernandez, I., Belabbas, B., Spletter, A., Rippl, M.: A proposal for multi-constellation advanced raim for vertical guidance. (09 2011)

[3] Brenner, M.: Integrated GPS/inertial fault detection availability. NAVIGATION: Journal of the Institute of Navigation **43**(2) (1996) 339–358

[4] Brown, R.G., Chin, G.Y. In: GPS RAIM: Calculation of Threshold and Protection Radius Using Chi-Square Methods – A Geometric Approach. Radio Technical Commission for Aeronautics (1998)

[5] GEAS Phase II: The GNSS evolutionary architecture study. Technical report (2010)

[6] Groves, P.D.: Principles of GNSS, Inertial, and Multisensor Integrated Navigation Systems. Artech House (2008)

[7] Joerger, M., Pervan, B.: Fault detection and exclusion using solution separation and chi-squared ARAIM. IEEE Transactions on Aerospace and Electronic Systems **52**(2) (2016) 726–742

[8] Kaňa, Z., Orejas, M., Soták, M., Duník, J.: Architectures for high integrity multi-constellation solution separation. In: Proceedings of the 27th International Technical Meeting of The Satellite Division of the Institute of Navigation, Tampa, FL (September 2014)

[9] Khalife, J., Maaref, M., Kassas, Z.M.: Opportunistic autonomous integrity monitoring for enhanced uav safety. IEEE Aerospace and Electronic Systems Magazine **38**(5) (2023) 34–44

[10] Lee, Y.C.: Analysis of range and position comparison methods as a means to provide gps integrity in the user receiver. In: Proceedings of the 42nd Annual Meeting of The Institute of Navigation, Seattle, WA, USA (1986)

[11] Orejas, M., Duník, J.: Hybrid DFMC GNSS/INS to support approach operations. In: Proceedings of the 2014 International Technical Meeting of The Institute of Navigation, San Diego, CA, USA (January 2014)

[12] Prol, F.S., Ferre, R.M., Saleem, Z., Välisuo, P., Pinell, C., Lohan, E.S., Elsanhoury, M., Elmusrati, M., Islam, S., Çelikbilek, K., Selvan, K., Yliaho, J., Rutledge, K., Ojala, A., Ferranti, L., Praks, J., Bhuiyan, M.Z.H., Kaasalainen, S., Kuusniemi, H.: Position, navigation, and timing (PNT) through low earth orbit (LEO) satellites: A survey on current status, challenges, and opportunities. IEEE Access **10** (2022) 83971–84002

[13] Prol, F.S., Bhuiyan, M.Z.H., Kaasalainen, S., Lohan, E.S., Praks, J., Çelikbilek, K., Kuusniemi, H.: Simulations of dedicated LEO-PNT systems for precise point positioning: Methodology, parameter analysis, and accuracy evaluation. IEEE Transactions on Aerospace and Electronic Systems (2024) 1–19

[14] Prol, F.S., Smirnov, A., Kaasalainen, S., Hoque, M.M., Bhuiyan, M.Z.H., Menzione, F.: The potential of LEO-PNT mega-constellations for ionospheric 3-D imaging: A simulation study. IEEE Journal of Selected Topics in Applied Earth Observations and Remote Sensing **16** (2023) 7559–7571

[15] RTCA DO-208: Minimum operational performance standards for airborne supplemental navigation equipment using global positioning system (GPS). Mops, Radio Technical Commission for Aeronautics, Washington, DC, USA (1991)

[16] Wang, K., El-Mowafy, A., Rizos, C.: Integrity monitoring for precise orbit determination of LEO satellites. GPS Solutions (32) (2022)

[17] Wang, K., El-Mowafy, A., Wang, W., Yang, L., Yang, X.: Integrity monitoring of PPP-RTK positioning; part II: LEO augmentation. Remote Sensing **14**(7) (2022)

[18] Wang, L., Chen, R., Xu, B., Zhang, X., Li, T., Wu, C.: The challenges of LEO based navigation augmentation system – lessons learned from Luojia-1A satellite. In Sun, J., Yang, C., Yang, Y., eds.: China Satellite Navigation Conference (CSNC) 2019 Proceedings, Singapore, Springer Singapore (2019) 298–310

[19] Young, R.S.Y., McGraw, G.A.: Fault detection and exclusion using normalized solution separation and residual monitoring methods. NAVIGATION **3** (2003) 151–169